Nuclear interference processes in the dissociation of H_2^+ in short vuv laser fields

Valery Mezoui Ndo,[1] Luc Owono Owono,[2] Bernard Piraux,[3] Samira Barmaki,[4] Morten Førre,[5] and Henri Bachau[6]

[1]*Centre de Physique Atomique, Moléculaire et Optique quantique (CEPAMOQ), Faculté des sciences, Université de Douala, P.O. Box 8580, Douala, Cameroon*

[2]*Department of Physics, Ecole Normale Supérieure, Université of Yaoundé I, B.P. 47 Yaoundé, Cameroon*

[3]*Institute of Condensed Matter and Nanosciences (IMCN), Université Catholique de Louvain, 2, Chemin du Cyclotron, Box L7.01.07, B-1348 Louvain-la Neuve, Belgium*

[4]*Secteur Sciences, Université de Moncton, Campus de Shippagan, 218 Boulevard J.-D. Gauthier, Shippagan, New Brunswick, Canada E8S 1P6*

[5]*Department of Physics and Technology, University of Bergen, N-5007 Bergen, Norway*

[6]*Centre des Lasers Intenses et Applications, Université Bordeaux 1-CNRS-CEA, 351 Cours de la Libération, F-33405 Talence Cedex, France*

(Received 30 January 2012; published 18 July 2012)

We use a $\mathcal{L}^2$-discretization technique for solving the time-dependent Schrödinger equation for H_2^+ interacting with a short vuv laser pulse, in the Born-Oppenheimer approximation. The calculations include the electronic three-dimensional and vibrational one-dimensional motions. In this approach, we use the prolate spheroidal coordinate system to describe the electronic functions and a basis of Laguerre and Legendre functions [Phys. Rev. A **71**, 053407 (2005)]. The vibrational motion is treated by using a basis of Sturmian functions. We consider the problem of two-photon dissociation of H_2^+ with photons ranging from 0.32 to 0.4 a.u corresponding to wavelengths from 143 to 114 nm. The initial vibrational wave packet results from a vertical (Franck-Condon) transition from the H_2 ground state towards a superposition of vibrational states in the $1s\sigma_g$ electronic state of H_2^+. The effects of various types of nuclear interference on the population of the dissociative channels $2s\sigma_g$ and $3d\sigma_g$ are discussed in detail. In addition, we show that for 0.32-a.u. photon energy, the interference effects in the $3d\sigma_g$ channel whose existence has been demonstrated previously [Phys. Rev. Lett. **102**, 123001 (2009)] can be observed in the total kinetic energy release spectrum.

DOI: 10.1103/PhysRevA.86.013416 PACS number(s): 33.80.Rv, 33.80.Gj, 82.53.Eb

I. INTRODUCTION

Current laser technology has opened up a new field of study namely the nonlinear response of matter to short and intense uv and vuv laser pulses. Sparked by experiments that have become feasible at intense high harmonics in the femtosecond regime (see e.g., Refs. [1–3]), theoretical interest for nonlinear processes at short wavelengths has just exploded. Among these processes, one of the most fundamental ones is undoubtedly the three-body Coulomb breakup. In the case of atoms, for instance, there has been a tremendous activity in predicting the removal by a few uv photons of two electrons from He (see Ref. [4] for a recent paper, and references therein). The study of the highly correlated dynamics of multiphoton double ionization of atoms poses real difficulties mostly because of the long-range nature of the Coulomb interaction between the electrons. In addition, the six-dimensional nature of the problem involving two-active electron atoms increases enormously the computing efforts that are required to calculate the relevant energy spectra and probabilities.

In the molecular context, a great deal of effort is made to unveil the various mechanisms of complete breakup of light molecules by a few uv photons. In that case, the main difficulties result from the complexity in accounting for both the electronic and nuclear degrees of freedom. Fundamental issues related to the interaction of light molecules with intense fields whose intensity exceeds 10^{12} W/cm^2 have been studied intensively (see Refs. [5,6] for reviews), but most of these studies were conducted in the near infrared (ir) (wavelength $\sim$800 nm) or in the visible-uv regime, at the time scale of several tens of fs. When the laser-molecule interaction is strong and many photons are emitted and/or absorbed during the reaction, the electronic structure is strongly perturbed (e.g., by the optical Stark shift effect). This leads to computational difficulties and, in some cases, to serious problems when extracting the basic mechanisms underlying the laser-molecule interaction under study. It is noteworthy that, using vuv fields, only few photons are involved at moderate intensities (10^{12}–10^{13} W/cm^2), while leaving the electronic structure much less perturbed than in the ir case.

Molecular processes are of particular interest in the femtosecond regime because the nuclear motion of light molecules typically occurs at this time scale. In this context, H_2^+ and H_2 (as well as D_2^+ and D_2) are ideal candidates to investigate the general mechanisms that govern multiphoton processes since they are accessible to an accurate theoretical description. Techniques using high-order harmonic generation provide laser light at high intensities in the femtosecond regime and experiments have already been performed in this domain (see Refs. [3,7] for a more recent publication). Recent theoretical investigations of laser molecule interactions in the vuv nonlinear regime have revealed new features occurring in the femtosecond time domain [8–10].

In this work, using $\mathcal{L}^2$-discretization techniques for solving the four-dimensional (4D) time-dependent Schrödinger equation (TDSE) of H_2^+, we study the problem of two-photon dissociation of the molecule in the photon energy range from 0.34 to 0.4 a.u. and laser pulse durations varying from 10 to 18 fs. Both the electronic 3D and vibrational 1D motions are included in the calculations, within the Born-Oppenheimer (B-O) approximation. In a precedent work [10], we

investigated a situation where the population is transferred coherently, via resonant one- and two-photon absorption, to the $2p\sigma_u$ and $3d\sigma_g$ potential curves, respectively. The $2p\sigma_u$ dissociative wave packet then moves rapidly to a large internuclear distance ($R \sim 10$ a.u.) where a second photon pumps population to the $3d\sigma_g$. The two paths leading to populating $3d\sigma_g$ interfere, resulting in a modulation of the kinetic energy release (KER) spectrum of the protons in the $3d\sigma_g$ dissociative channel. We show that the modulation of the KER spectrum of the protons also occurs in the case of the $2s\sigma_g$ channel, but the origin of the modulation is now different. Based on this finding, various interference mechanisms in the dissociation dynamics of H_2^+ are discussed in detail. In the case of a photon energy of 0.32 a.u. investigated in Ref. [10], we show that the $2s\sigma_g$ channel is much less populated than the $3d\sigma_g$ one. As a result, the interference effects should be observable experimentally in the total KER spectrum. Such a study of the dissociation of H_2^+ which is of current interest both from the methodological and the physical points of view [11,12], is also a strong test of the reliability of our numerical approach since it involves dipole couplings at large internuclear distances.

Our paper is organized as follows. The second section is devoted to a brief discussion of our theoretical approach. We first present the general formulation of the problem. Then, we analyze the electronic and vibrational structures of H_2^+. The section ends by some considerations over the time propagation of the vibrational wave packets in the presence of the external pulsed field. The next section is devoted to the results for the KER spectrum of the protons in both the $2s\sigma_g$ and the $3d\sigma_g$ dissociative channels. Unless stated otherwise, atomic units are used throughout this paper.

II. THEORY

In this section, we describe our numerical approach for solving, within the Born-Oppenheimer (B-O) approximation, the four-dimensional TDSE for H_2^+ in interaction with a laser pulse. We treat the electronic motion in its full dimensionality (3D) and also include the one-dimensional vibrational motion. Concerning the electronic structure, the problem is treated as in Ref. [13] (i.e., we use the prolate spheroidal coordinate system to describe the electronic motion in a basis of Laguerre and Legendre functions). The latter approach has been shown to be very efficient. Its pertinence has been thoroughly discussed in the literature [13] (see other references therein) where it was used with fixed nuclei. In our opinion it represents an interesting alternative to B-spline functions, currently used in a similar context [8,14,15] (see Ref. [16] for a review). The vibrational motion is treated by using a basis of Coulomb Sturmian functions. These functions have been shown to be very efficient in the case of atomic systems [17]. They have in particular the potential to describe diffuse states (e.g., Rydberg states) and their use to treat two-active electron systems allowed the very accurate calculation of the energy and width of high-lying doubly excited states in He [18–20]. In the present context, the Sturmian functions are particularly adapted to describe high-lying vibrational states just below or above the dissociation threshold.

A. Basic formulation

In the present calculations, we use the B-O approximation and neglect the mass polarization terms as well as relativistic effects. Since the time scale associated with the rotational motion of the molecule is much longer than the duration of the vuv pulses considered in this contribution, it is a good approximation to neglect the rotational structure of the molecule. Under these conditions, the stationary Schrödinger equation (SSE) for H_2^+ writes as follows:

$$\left(-\frac{1}{2\mu}\nabla_R^2 + H_e(\vec{r},R)\right)\Psi_{n,\nu}(\vec{r},R) = W_{n,\nu}\Psi_{n,\nu}(\vec{r},R). \quad (1)$$

Here $\vec{r}$ is the position vector of the electron with respect to the center of mass of the two nuclei and R is the internuclear distance. The first term between the brackets is the operator associated with the relative kinetic energy of the nucleus while the second term is the electronic Hamiltonian that contains all the potential energy terms. $W_{n,\nu}$ is the total energy of the molecule, the indices n and ν referring to the electronic and vibrational quantum numbers, respectively. Since within the B-O approximation, electronic and nuclear motions can be separated, the stationary wave function, the solution of Eq. (1), can be written as a product of electronic and vibrational wave functions:

$$\Psi_{n,\nu}(\vec{r},R) = \frac{\chi_{n,\nu}(R)}{R}\psi_n(\vec{r},R). \quad (2)$$

The electronic wave function is the solution of the equation,

$$H_e\psi_n(\vec{r},R) = E_n\psi_n(\vec{r},R), \quad (3)$$

with the electronic Hamiltonian,

$$H_e = -\frac{1}{2}\nabla^2 + V(r) + \frac{Z^2}{R}. \quad (4)$$

Z is the charge of each nucleus and $V(r)$ is the attractive Coulomb potential experienced by the electron. It is given by

$$V(r) = V_1(r) + V_2(r) = -\frac{Z}{r_1} - \frac{Z}{r_2}, \quad (5)$$

where $\vec{r}_1$ and $\vec{r}_2$ are the position vectors of the electron with respect to each of the nuclei. The vibrational wave function satisfies the following equation:

$$[H_\nu(R) - W_{n,\nu}]\chi_{n,\nu}(R) = 0. \quad (6)$$

As mentioned above, $W_{n,\nu}$ is the total energy of the molecule for the vibrational state ν in the electronic state n. The Hamiltonian $H_\nu(R)$ writes

$$H_\nu(R) = T(R) + E_n(R) = -\frac{1}{2\mu}\frac{d^2}{dR^2} + \frac{J(J+1)}{2\mu R^2} + E_n(R), \quad (7)$$

where $T(R)$ is the operator associated with the kinetic energy of the nuclei, $E_n(R)$ is the B-O potential energy curve of the nth electronic state, μ is the reduced mass of the nuclei, and J is the total orbital angular momentum (here $J = 0$).

B. The electronic structure of H_2^+

In order to solve Eq. (3) for the electronic wave function, it is convenient to use the system of prolate spheroidal coordinates

(ξ,η,φ) in which the electronic Hamiltonian (4) is separable. φ is the rotation angle around the internuclear axis. It varies between 0 and 2π. The variables ξ and η are defined as

$$\xi = (r_1 + r_2)/R, \tag{8}$$

$$\eta = (r_1 - r_2)/R, \tag{9}$$

with $1 \leqslant \xi \leqslant +\infty$ and $-1 \leqslant \eta \leqslant 1$. In this new system of coordinates, the electronic Hamiltonian H_e takes the following form:

$$H_e = -\frac{2}{R^2(\xi^2-\eta^2)}\left[\frac{\partial}{\partial\xi}(\xi^2-1)\frac{\partial}{\partial\xi} + \frac{\partial}{\partial\eta}(1-\eta^2)\frac{\partial}{\partial\eta} + \left(\frac{1}{\xi^2-1}+\frac{1}{1-\eta^2}\right)\frac{\partial}{\partial\varphi^2} + 2ZR\xi\right] + \frac{Z^2}{R}. \tag{10}$$

In order to solve Eq. (3) for a given value of the parameter R, the electronic wave function is expanded as follows:

$$\psi(\xi,\eta,\theta;R) = \sum_{m,\mu,\nu} a_{m\mu\nu} U_\nu^m(\xi) V_\mu^m(\eta) \frac{e^{im\theta}}{\sqrt{2\pi}}. \tag{11}$$

m is the projection of the electronic angular momentum along the z axis that coincides with the internuclear axis. It takes the values $0,\pm1,\pm2,\ldots$ and it is conserved provided that the axial symmetry is preserved. The two indices ν and μ give the number of zeros of the functions $U_\nu^m(\xi)$ and $V_\mu^m(\eta)$. They take the values $\mu = |m|,|m|+1,\ldots$ and $\nu = |m|,|m|+1,\ldots$. $a_{m\mu\nu}$ are the expansion coefficients of the wave function. The basis functions $U_\nu^m(\xi)$ and $V_\mu^m(\eta)$ are defined as in Lagmago *et al.* [13]:

$$U_\nu^m(\xi) = N_\nu^m e^{-\alpha(\xi-1)}(\xi^2-1)^{|m|/2} L_{\nu-|m|}^{2|m|}[2\alpha(\xi-1)], \tag{12}$$

and

$$V_\mu^m(\eta) = M_\mu^m P_\mu^m(\eta), \tag{13}$$

where $L_p^q(x)$ denotes the Laguerre polynomials and $P_p^q(x)$ the associated Legendre function of the first kind. Note that the functions $U_\mu^m(\xi)$ depend on a dilation parameter α which determines their range. The normalization conditions are

$$\int_1^{+\infty} U_\mu^m(\xi)\left(\frac{\xi-1}{\xi+1}\right)^{|m|} U_\nu^m(\xi)d\xi = 1, \tag{14}$$

and

$$\int_{-1}^{+1} V_\mu^m(\eta) V_\mu^m(\eta) d\eta = 1, \tag{15}$$

which lead to the following expressions for the normalization constants:

$$M_\mu^m = \sqrt{\left(\frac{1}{2}+\mu\right)\frac{(\mu-m)!}{(\mu+m)!}}, \tag{16}$$

and

$$N_\nu^m = \sqrt{(2\alpha)^{2|m|+1}\frac{(\nu-|m|)!}{(\nu+|m|)!}}. \tag{17}$$

By substituting expressions (12) and (13) into Eq. (3) and projecting on the basis functions on the left, Eq. (3) transforms into the generalized matrix eigenvalue problem,

$$\mathbf{H}_e\mathbf{\Psi} = E\mathbf{S}\mathbf{\Psi}, \tag{18}$$

where $\mathbf{\Psi}$ is the vector representation of the wave function, $\mathbf{S}$ is the overlap matrix, and $\mathbf{H}_e$ is the electronic Hamiltonian matrix. Details on the evaluation in compact form of the matrix elements of $\mathbf{S}$ and $\mathbf{H}$ are given in Ref. [13]. In fact, all these matrix elements can be expressed in terms of product of one-dimensional integrals. In the present contribution, we evaluate these integrals numerically by means of a Gauss-Laguerre quadrature which gives accurate and in principle exact results.

The resolution of the generalized eigenvalue problem (18) yields both bound states and discretized continuum states. Their accuracy depends on the number of basis functions as well as on the value of the dilation parameter α.

Table I gives the values of the potential energy curves corresponding to the four first electronic molecular states for $m = 0$ at various internuclear distances R. The states are labeled with the quantum number μ and m defined above. In the case of the united atom limit, the atomic angular momentum $l = \mu + m$. In all our calculations, the electronic states of H_2^+ have been represented with the following basis parameters: $\alpha = 1.5$, $\mu_{\max} = 20$, $\nu = 50$, and $m = 0$ in a box of radial length of 40 a.u. By changing the number of basis functions and the value of α (from 0.5 to 1.5), we have checked that this basis set leads to practically converged energies in the Franck-Condon region. Figure 1 shows the four first potential energy curves of σ symmetry for H_2^+ as a function of the internuclear distance.

TABLE I. Energy (in a.u.) of the $1s\sigma_g$, $2p\sigma_u$, $3d\sigma_g$, and $2s\sigma_g$ electronic states of H_2^+ for various internuclear distances R (in a.u.).

R	$1s\sigma_g$	$2p\sigma_u$	$3d\sigma_g$	$2s\sigma_g$
1	−0.45178631337844188	0.43518685067772556	0.77734132942080780	0.57712214175170917
2	−0.60263421449494381	−0.16753439220238683	0.26422238152159605	0.13913512466373507
3	−0.57756286404892043	−0.36808500003988742	0.0758290294366485151	0.0144462795334254594
4	−0.54608488371094044	−0.44555063936041733	−0.0357237904797696390	−0.0385148674574864736
5	−0.52442029512349020	−0.47729161322515518	−0.10601307783608663	−0.0655058146771253652
6	−0.51196904791010645	−0.49064389229696509	−0.14582816013612568	−0.0808879228148097762
7	−0.50559400001171040	−0.49627171206834358	−0.16556342053472303	−0.0904222566648646975
8	−0.50257036607306194	−0.49860601447265451	−0.17351164140955100	−0.0967773328649080555
9	−0.50119534649749342	−0.49954381723892127	−0.17500068978131425	−0.10130135619564577
10	−0.50057824313448462	−0.49990091663882358	−0.17311743737431354	−0.10471062557910241

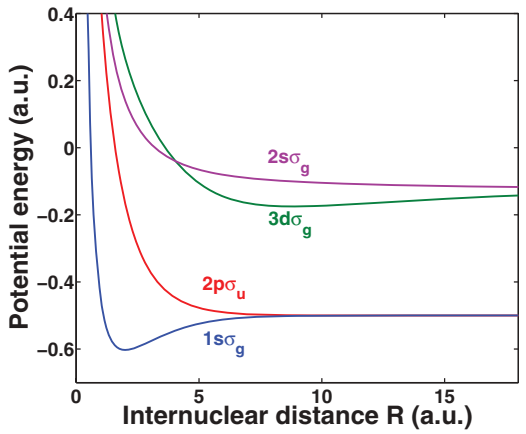

FIG. 1. (Color online) First four potential energy curves of σ symmetry for H_2^+ as a function of the internuclear distance.

C. The vibrational structure of H_2^+

Once the electronic energy curves have been obtained, the vibrational levels can be determined with a view to computing the KER spectrum of the protons. In order to solve Eq. (6), we expand the functions $\chi_{n,v}(R)$ in a basis of Sturmian functions,

$$\chi_{n,v}(R) = \sum_{\mathrm{v}=1}^{\mathrm{v}_{\max}} c_{n,v}^{\mathrm{v}} S_{\mathrm{v}l}^{\kappa}(R), \tag{19}$$

$c_{n,v}^{\mathrm{v}}$ being the expansion coefficients. Furthermore, the Sturmian function $S_{\mathrm{v}l}^{\kappa}(R)$ is given by

$$S_{\mathrm{v}l}^{\kappa}(R) = N_{\mathrm{v}l}^{\kappa}\ R^{l+1} e^{-\kappa R}\ L_{\mathrm{v}-l-1}^{2l+1}(2\kappa R), \tag{20}$$

$L_{\mathrm{v}-l-1}^{2l+1}(2\kappa R)$ denoting a Laguerre polynomial. These Sturmian functions form a complete and discrete set of functions. The normalization factor $N_{\mathrm{v}l}^{\kappa}$ is given by

$$N_{\mathrm{v}l}^{\kappa} = \sqrt{\frac{k}{\mathrm{v}}}\ (2\kappa)^{l+1} \left[\frac{(n-l-1)!}{(n+l)!}\right]^{\frac{1}{2}}. \tag{21}$$

It results from the condition,

$$\int_0^{\infty} S_{\mathrm{v}l}^{\kappa}(R) S_{\mathrm{v}l}^{\kappa}(R) dR = 1. \tag{22}$$

In order to calculate the vibrational wave functions we have to solve the following generalized eigenvalue problem,

$$\mathbf{H}_v \mathbf{X} = W_n \mathbf{B} \mathbf{X}, \tag{23}$$

where $\mathbf{H}_v$ is the matrix associated with the Hamiltonian (7), and $\mathbf{B}$ is the overlap matrix. $\mathbf{X}$ is the vector representation of a vibrational eigenstate in the potential well associated with the nth electronic state and W_n is the total energy of the molecule in the corresponding vibrational eigenstate. In the following, we have calculated the vibrational levels (i.e., the total energy $W_{n,v}$) of H_2^+ by means of a basis of 200 Sturmian functions for each electronic state in a radial box the size of which is of the order of 40 a.u. The value of κ is set equal to 10. Results converge well for values of κ running from 5 to 15 for the vibrational states and for values of α running from 0.4 to 1.5 for the electronic states. It is worth stressing that since κ and α represent dilation parameters, choosing $\kappa \gg \alpha$ means that the vibrational states are defined in a much smaller box than the electronic ones. Table II shows vibrational levels for some electronic states of interest.

Note that the discrete nature of the continuum states ($2p\sigma_u$, $3d\sigma_g$, and $2s\sigma_g$) is a consequence of the finite box size. The eigenvalues that are above the dissociating limit correspond to vibrational continuum states. The wave function associated with these continuum states are normalized to unity. The calculation of probability densities requires the evaluation of the density of these vibrational continuum states that is given by

$$\rho_{n,v} = \left|\frac{2}{W_{n,v-1} - W_{n,v+1}}\right|. \tag{24}$$

D. Time propagation

In this contribution, we want to calculate the KER spectrum of H_2^+ in the two dissociative channels $3d\sigma_g$ and $2s\sigma_g$. The

TABLE II. Vibrational energy levels $W_{n,v}$ (in a.u.) with n referring to the electronic states $1s\sigma_g$, $2p\sigma_u$, $3d\sigma_g$, and $2s\sigma_g$.

v	$W_{1s\sigma_g,v}$	$W_{2p\sigma_u,v}$	$W_{3d\sigma_g,v}$	$W_{2s\sigma_g,v}$
0	−0.59739590504034934	−0.49995157541876278	−0.17405758494098561	−0.12085739630007920
1	−0.58740832106458885	−0.49973323999886343	−0.17211168004231550	−0.12049750167315978
2	−0.57800090770993884	−0.49947966349092193	−0.17021215208430321	−0.12010502133287969
3	−0.56915441225629193	−0.49919980968814204	−0.16835807408306036	−0.11969333761121072
4	−0.56085258512797931	−0.49889840328164703	−0.16654857545729765	−0.11926845469016549
5	−0.55308210091594778	−0.49857855816151120	−0.16478284147348360	−0.11883307436845167
6	−0.54583252393195236	−0.49824252637509103	−0.16306011289728967	−0.11838838692697330
7	−0.53909631986400242	−0.49789203430923201	−0.16137968585547222	−0.11793484463134410
8	−0.53286891683376758	−0.49752845947388680	−0.15974091190310702	−0.11747253604411174
9	−0.52714882119138329	−0.49676640819062162	−0.15814319830775259	−0.11700138551253317
10	−0.52193779581514843	−0.49636969643233075	−0.15658600855574339	−0.11652126452553363
11	−0.51724111148589125	−0.49596350443057241	−0.15658600855574339	−0.11603205282582872
12	−0.51306788460879382	−0.49554845214201909	−0.15506886306621456	−0.11553366882124047
13	−0.50943151497903627	−0.49512508945548278	−0.15359134013338335	−0.11502608115397200
14	−0.50635022688110110	−0.49469390829131415	−0.15215307708316989	−0.11450930922719098

KER spectrum is obtained by solving numerically the TDSE governing the laser-molecule interactions,

$$i\frac{\partial}{\partial t}\Phi(\vec{r},R,t) = [H + V(t)]\Phi(\vec{r},R,t), \tag{25}$$

where H is the Hamiltonian given by the term between parentheses in Eq. (1), and $V(t)$ is the laser-molecule interaction potential which can be written as

$$V(t) = \vec{E}(t)\cdot\vec{r}, \tag{26}$$

in the length gauge, and

$$V(t) = \vec{A}(t)\cdot\vec{p}, \tag{27}$$

in the velocity gauge. Here $\vec{E}(t)$ is the electric field that is assumed to be polarized along the internuclear axis, and $\vec{A}(t)$ is the corresponding vector potential. It is defined as follows:

$$\vec{A}(t) = A_0 f(t)\cos(\omega t)\vec{e}_z, \tag{28}$$

where ω is the photon energy in a.u., A_0 is the amplitude, and the pulse envelope $f(t)$ is given by

$$f(t) = \begin{cases} \cos^2\left(\frac{\pi}{T}t\right), & |t| < \frac{T}{2}, \\ 0, & |t| \geqslant \frac{T}{2}. \end{cases} \tag{29}$$

T is the total duration of the pulse. In order to calculate the electric field, we use the usual relation,

$$\vec{E}(t) = -\frac{\partial}{\partial t}\vec{A}(t). \tag{30}$$

Equation (25) is integrated over the whole pulse duration T in the basis of the eigenstates of the Hamiltonian H. Note that in order to facilitate the time propagation, it is convenient to use the interaction picture. In this picture, the Schrödinger equation [Eq. (25)] writes

$$i\frac{\partial}{\partial t}\Phi_I(\vec{r},R,t) = [e^{iH(t-t_0)}V(t)e^{-iH(t-t_0)}]\Phi_I(\vec{r},R,t), \tag{31}$$

where the index "I" refers to the interaction picture, and

$$\Phi_I(\vec{r},R,t) = e^{iH(t-t_0)}\Phi(\vec{r},R,t). \tag{32}$$

In the present context, the solution $\Phi(\vec{r},R,t)$ is written as a superposition of four products of electronic and nuclear wave functions. More precisely, we model the nuclear dissociation dynamics by writing the complete wave function as a superposition of the four electronic eigenfunctions $1s\sigma_g$, $2p\sigma_u$, $3d\sigma_g$, and $2s\sigma_g$, weighted by the corresponding nuclear amplitudes [14],

$$\begin{aligned}\Phi(\vec{r},R,t) = &\sum_{\nu=1}^{N_{\rm vib}} a_{1s\sigma_g,\nu}(t)\phi_{1s\sigma_g}(\vec{r},R)\frac{\chi_{1s\sigma_g,\nu}(R)}{R} \\ &+ \sum_{\nu'=1}^{N_{\rm vib}} a_{2p\sigma_u,\nu'}(t)\phi_{2p\sigma_u}(\vec{r},R)\frac{\chi_{2p\sigma_u,\nu'}(R)}{R} \\ &+ \sum_{\nu''=1}^{N_{\rm vib}} a_{3d\sigma_g,\nu''}(t)\phi_{3d\sigma_g}(\vec{r},R)\frac{\chi_{3d\sigma_g,\nu''}(R)}{R} \\ &+ \sum_{\nu'''=1}^{N_{\rm vib}} a_{2s\sigma_g,\nu'''}(t)\phi_{2s\sigma_g}(\vec{r},R)\frac{\chi_{2s\sigma_g,\nu'''}(R)}{R}, \end{aligned} \tag{33}$$

where $a_{1s\sigma_g,\nu}(t)$, $a_{2p\sigma_u,\nu'}(t)$, $a_{3d\sigma_g,\nu''}(t)$, and $a_{2s\sigma_g,\nu'''}(t)$ are the probability amplitudes of the vibrational states corresponding to the first four potential curves in the $m = 0$ symmetry. ν, ν', ν'', and ν''' label both bound and continuum vibrational states for each potential curve. In this basis, the elements of the matrix associated with the interaction $V(t)$ write

$$V(t)_{n,\nu,n',\nu'} = E(t)\int_0^{+\infty}\chi_{n,\nu}(R)\chi_{n',\nu'}(R)D_{n,n'}(R)dR, \tag{34}$$

where $D_{n,n'}(R)$ represents the dipole coupling between the electronic states n and n'. It is important to note that the eigenvectors of the electronic Hamiltonian are defined within an arbitrary phase factor and there is no guarantee that this phase factor will stay constant when the electronic Hamiltonian is diagonalized at various internuclear distances. Obviously, this has important consequences for the calculation of the dipole coupling term $D_{n,n'}(R)$. An additional difficulty is that the sign of the coupling term $D_{n,n'}(R)$ may change "naturally." In order to overcome this difficulty, we proceed as follows. Assuming that the value of $D_{n,n'}(R)$ is known and that we want to calculate $D_{n,n'}(R+\Delta R)$, we first consider the following quantity:

$$S_n(R,R+\Delta R) = \int d\vec{r}\ \psi_n(\vec{r},R)\ \psi_n(\vec{r},R+\Delta R). \tag{35}$$

For ΔR sufficiently small, we expect that $S_n(R,R+\Delta R) \simeq \pm 1$. If $S_n(R,R+\Delta R)$ is approximately equal to 1, it is assumed that the phase does not change. On the contrary, if $S_n(R,R+\Delta R)$ is approximately equal to -1, the phase of ψ_n has changed. Similarly, we also evaluate $S_{n'}(R,R+\Delta R)$ to check whether the phase of $\psi_{n'}$ has changed. In this way, it is possible to check where a change of sign occurs and, after a careful analysis of the dipole couplings in that region, if it is artificial or not.

By inserting the time-dependent wave function (33) in the TDSE (25), we obtain a system of coupled first-order differential equations for the probability amplitudes which can be solved by using standard numerical techniques. The initial wave packet $\Phi(\vec{r},R,t=0)$ of H_2^+ is obtained by assuming that a direct vertical Franck-Condon transition from the vibrational ground state of H_2 takes place at $t = 0$, in such a way that this ground vibrational state can be projected onto a complete set of B-O vibrational states of H_2^+ in its ground electronic state $1s\sigma_g$. Consequently, we have

$$\Phi(\vec{r},R,t=0) = \sum_{\nu=1}^{N_{\rm vib}} a_{1s\sigma_g,\nu}(t=0)\phi_{1s\sigma_g}(\vec{r},R)\frac{\chi_{1s\sigma_g,\nu}(R)}{R}, \tag{36}$$

where the coefficients $a_{1s\sigma_g,\nu}(t=0)$ are given by

$$a_{1s\sigma_g,\nu}(t=0) = \int \chi_{1s\sigma_g,\nu}(R)\chi^{H_2}_{\nu=0}(R)dR, \tag{37}$$

and $\chi^{H_2}_{\nu=0}(R)$ is the wave function associated with the vibrational ground state of H_2. Note that the modulus square of the above coefficient is nothing else than the Franck-Condon factor.

In order to evaluate the KER spectrum in various dissociation channels, we calculate the following probability

density:

$$\frac{dP}{dW_{n,\nu}} = 2\frac{\left|a_{n,\nu}\left(\frac{T}{2}\right)\right|^2}{|W_{n,\nu+1} - W_{n,\nu-1}|}. \tag{38}$$

The vibrational energy $W_{n,\nu}$ is the center-of-mass kinetic energy of the outgoing protons. An important technical aspect of our SSE and TDSE calculations is the choice of the box size that has to be compatible with the physical boundary, namely the internuclear distance of the diatomic molecule. We use the following empirical formula $R = \frac{X}{2\kappa}$ where X is a Gauss-Laguerre quadrature abscissa, κ is the Sturmian nonlinear parameter [see Eq. (20)], and R the internuclear distance. If we increase the basis size or the number of Sturmian functions, X takes increasingly large values. This leads to out-of-range internuclear distances R. We then lose precision on vibrational functions and problems of divergence occur. To overcome this, κ must take relatively big values with a view to keeping reasonable internuclear distances R. Big values of κ also lead to the very high density of continuum states necessary to correctly describe the continuum spectrum. In fact, the separation between discretized vibrational states must be smaller than the spectral width $\Delta\omega \approx 4\pi/T$. In other words, the size of the box must be chosen so that the condition $\Delta W_{n,\nu} \lesssim \Delta\omega$ is fulfilled. This condition ensures that the vibrational wave packet does not reach the limit of the vibrational box before the end of the pulse. In the case of the $2p\sigma_u$ dissociative channel, κ is equal to 15, the number of vibrational states taken into account is 150 and the box size is 18.5 a.u. In the case of the $3d\sigma_g$ channel, κ is equal to 21, the number of vibrational states is 225 and the box size is 20 a.u. Finally, for the $2s\sigma_g$ channel, the value of κ is equal to 23, the number of vibrational states is 300 and the box size is 24.3 a.u.

III. RESULTS AND DISCUSSION

Our objective in this contribution is twofold. First, we want to revisit the problem of the vibrational wave-packet interferences (VWPI) in the $3d\sigma_g$ dissociative channel of H_2^+, treated in Ref. [10] and extend our analysis to the $2s\sigma_g$ channel. In parallel, we want to check the accuracy of our spectral approach based on Sturmian functions. As mentioned before, this accuracy relies on the appropriate choice of the nonlinear parameter κ which in turn determines the number and the density of vibrational states in the continuum. Comparing the results of our present calculations with those obtained with B splines should give a clear indication of this accuracy.

A. $3d\sigma_g$ dissociative channel

Let us start by describing the mechanism that leads to the VWPI process in the $3d\sigma_g$ dissociative channel. It is sketched in Fig. 2. A wave packet created at time $t = 0$ on the $1s\sigma_g$ electronic potential curve interacts with a short, soft uv femtosecond laser pulse. At $R_1 \approx 2.4$ a.u. and $R_2 \approx 3.1$ a.u., population is transferred coherently via resonant one- and two-photon absorption to the $2p\sigma_u$ and $3d\sigma_g$ curves, respectively. If the pulse duration is sufficiently long, the vibrational wave packet that moves on the $2p\sigma_u$ curve will reach $R = R_3 \approx 8.6$ a.u. where a second photon may be absorbed leading to a transition towards the $3d\sigma_g$ and to a VWPI in this channel.

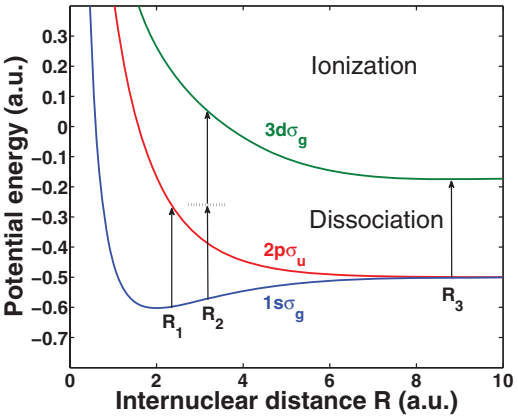

FIG. 2. (Color online) Sketch of a vibrational wave-packet interference process in the $3d\sigma_g$ dissociation channel of H_2^+. A wave packet created at time $t = 0$ on the $1s\sigma_g$ electronic potential curve interacts with a short, soft uv femtosecond laser pulse. At $R_1 \sim 2.4$ a.u. and $R_2 \sim 3.1$ a.u. population is transferred coherently via one- and two-photon absorption, to the $2p\sigma_u$ and the $3d\sigma_g$ curves, respectively. In the dissociative channel $2p\sigma_u$, a wave packet moves rapidly to $R_3 \sim 8.6$ a.u. where a second photon pumps population to the $3d\sigma_g$ energy curve leading to a vibrational wave-packet interference.

In Fig. 3, we show the KER spectrum of the protons in the $3d\sigma_g$ dissociative channel. We use a femtosecond laser pulse of central frequency $\omega = 0.32$ a.u. (corresponding to a wavelength of 142 nm) and peak intensity $I = 10^{12}$ W/cm^2. Six different total pulse durations ranging from 10 to 16 fs are considered. We assume that the initial vibrational wave packet at $t = 0$ is of the Franck-Condon type. The calculations have been performed by means of our spectral approach based on Sturmian functions. About 250 vibrational states are included. The results are stable for values of the nonlinear parameter κ ranging from 17 to 23 and are in perfect agreement with those obtained with a spectral method based on B splines as in Ref. [10]. The interference of wave packets leads to a double peak structure except for the shortest pulse duration where it disappears. In this latter case, the wave packet that

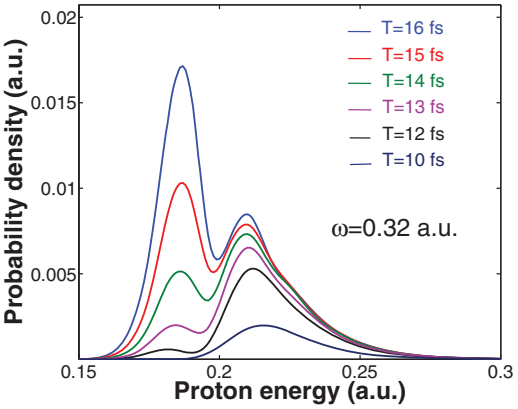

FIG. 3. (Color online) Kinetic energy release spectrum of the protons in the $3d\sigma_g$ dissociative channel obtained with a femtosecond laser pulse of central frequency $\omega = 0.32$ a.u. and peak intensity $I = 10^{12}$ W/cm^2. Six different pulse durations are considered. The initial vibrational wave packet at $t = 0$ is assumed to be of the Franck-Condon type.

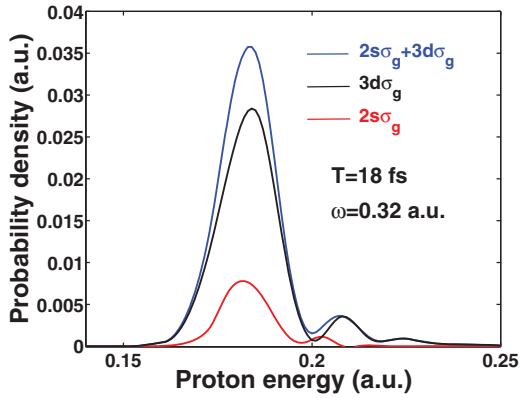

FIG. 4. (Color online) Kinetic energy release spectrum of the protons obtained with a femtosecond laser pulse of central frequency $\omega = 0.32$ a.u. and peak intensity $I = 10^{12}$ W/cm^2. The total pulse duration is 18 fs and the initial vibrational wave packet at $t = 0$ is assumed to be of the Franck-Condon type. The red curve corresponds to a calculation including the contribution of the $2s\sigma_g$ channel only. The black curve is obtained by including the contribution of the $3d\sigma_g$ channel only, while the blue curve is the sum of both contributions.

moves on the $2p\sigma_u$ curve does not have the time to reach the interatomic distance R_3 during the interaction with the pulse. At this stage, we can argue that in the presence of the field, the wave packet that oscillates (with a period close to 15 fs [21]) in the $1s\sigma_g$ channel can lead to the production at a later time of a second wave packet in the $3d\sigma_g$ dissociative channel. Subsequently, the two wave packets will interfere in this $3d\sigma_g$ channel. In principle, this second mechanism of VWPI should also contribute to the interference pattern observed in the KER spectrum of the protons. However, by artificially suppressing the $2p\sigma_u$-$3d\sigma_g$ coupling around $R = R_3$, the interference pattern we observe in the KER of the protons disappears. This rules out this second mechanism at least in the case of the $3d\sigma_g$ channel provided the pulses are not too long.

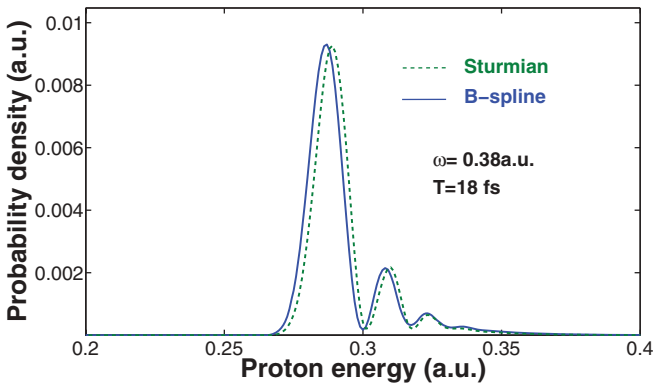

FIG. 5. (Color online) Kinetic energy release spectrum of the protons in the $2s\sigma_g$ dissociative channel obtained with a femtosecond laser pulse of central frequency $\omega = 0.38$ a.u. and peak intensity $I = 10^{12}$ W/cm^2. The pulse duration is 18 fs. The initial vibrational wave packet at $t = 0$ is assumed to be of the Franck-Condon type. Two calculations have been performed: the green dashed curve is our results obtained with Sturmian functions and the blue curve is our results obtained with B splines.

From the experimental point of view, it is impossible to separate the contributions from the various dissociative channels by only observing the KER of the protons. In addition, it is not clear whether the interference pattern will subsist when, in the present case, the contributions of the $2s\sigma_g$ and $3d\sigma_g$ are taken into account in the calculation of the KER spectrum of the protons. The results are shown in Fig. 4 for the same frequency ($\omega = 0.32$ a.u.) and peak intensity ($I = 10^{12}$ W/cm^2) as in Fig. 3. The total duration of the pulse is 18 fs and the initial vibrational wave packet is of the Franck-Condon type. We clearly see that the interference pattern subsists. It should therefore be observable experimentally.

B. $2s\sigma_g$ dissociative channel

In this subsection, we analyze in detail the contribution of the $2s\sigma_g$ channel to the KER of the protons, and examine more in depth the validity of our spectral method based on the Sturmian functions. In Fig. 5, we depict the KER spectrum of the protons in the $2s\sigma_g$ dissociation channel. The central frequency ω of the laser pulse is equal to 0.38 a.u. (corresponding to a wavelength of 120 nm) and the peak intensity 10^{12} W/cm^2. The duration T of the pulse is 18 fs, and the initial wave packet is of the Franck-Condon type. The

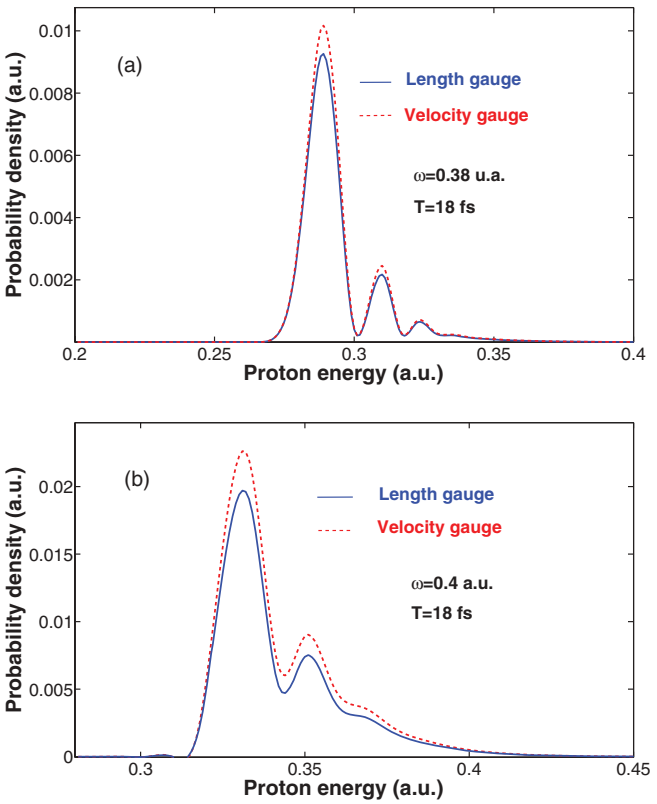

FIG. 6. (Color online) Kinetic energy release spectra of the protons in the $2s\sigma_g$ dissociative channel obtained with a femtosecond laser pulse of peak intensity $I = 10^{12}$ W/cm^2 and a central frequency (a) $\omega = 0.38$ a.u. and (b) $\omega = 0.40$ a.u. The pulse duration is equal to 18 fs. The initial vibrational wave packet at $t = 0$ is assumed to be of the Franck-Condon type. The calculations have been performed with Sturmian functions in the velocity gauge (blue curves) and the length gauge (red dashed curves).

green dashed curve has been obtained with Sturmian functions. More precisely, 310 Sturmians have been used to describe the vibrational states in each electronic state. The nonlinear parameter κ is in that case equal to 23 and the size of the nuclear box is about 25 a.u. In fact, for values of κ ranging from 21 to 27, the results are stable. The blue curve has been obtained by using, for each electronic state, 350 B splines of order 7 in a nuclear box of 30.5 a.u. The agreement between both curves is very good except for a very tiny shift of the main peak. Note that for $\kappa = 23$, the range of the Sturmian functions is in general rather short unless the index of the function becomes large. It is also worth mentioning that when the calculations are performed in a well-defined box, as is the case for the B splines, there is no well defined energy threshold. In Fig. 6, we analyze the gauge dependence of our results obtained with the Sturmian functions for a 18 fs pulse of 10^{12} W/cm^2 peak intensity. Two different frequencies are considered: (a) $\omega = 0.38$ a.u. and (b) $\omega = 0.4$ a.u. As before, the initial vibrational wave packet at $t = 0$ is assumed to be of Franck-Condon type. The blue curves have been obtained within the velocity gauge and the red dashed ones within the length gauge. Except for small differences (more pronounced for $\omega = 0.4$ a.u.) around the maxima, the agreement between the blue and red dashed curves is rather good. Note that a perfect agreement is not expected since the problem is solved within the B-O approximation.

In Fig. 7, we analyze the kinetic energy release spectra of the protons in the $2s\sigma_g$ dissociative channel for different frequencies and pulse durations. All pulses have a peak intensity of 10^{12} W/cm^2. We consider four different values of the frequency: 0.32 a.u., 0.34 a.u., 0.36 a.u., and 0.38 a.u., as well as three pulse durations, 10 fs, 14 fs, and 18 fs. As before, the initial vibrational wave packet at time $t = 0$ is of the Franck-Condon type. The results clearly show that interferences characterized by a double peak structure, occur for a broad range of frequencies provided that the pulse is sufficiently long. For the shortest pulse duration, namely 10 fs, the interferences disappear at all frequencies. By contrast with the $3d\sigma_g$ dissociative channel, the mechanism that leads to the interference pattern is not so clear in the $2s\sigma_g$ channel case. By switching off the $2p\sigma_u$-$2s\sigma_g$ coupling at larger internuclear distances, where the resonant one-photon transition from the $2p\sigma_u$ to the $2s\sigma_g$ may occur, the interference pattern still subsists. This seems to indicate that the second VWPI mechanism

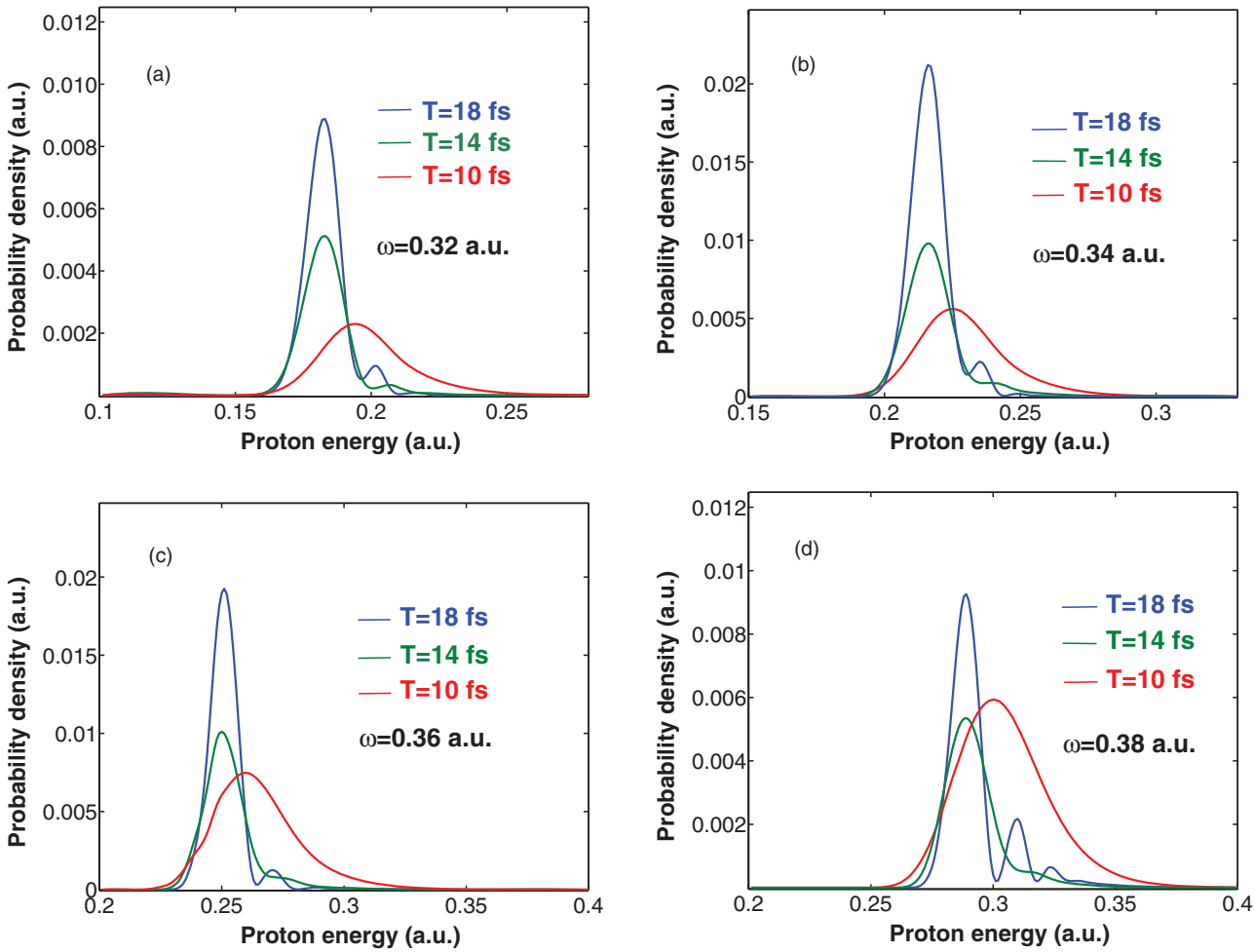

FIG. 7. (Color online) Kinetic energy release spectra of the protons in the $2s\sigma_g$ dissociative channel obtained with a femtosecond laser pulse of peak intensity $I = 10^{12}$ W/cm^2. Four central frequencies are considered: (a) 0.32 a.u., (b) 0.34 a.u., (c) 0.36 a.u., and (d) 0.38 a.u. In each case, three total pulse durations are considered: 10 fs, 14 fs, and 18 fs. The initial vibrational wave packet at $t = 0$ is assumed to be of the Franck-Condon type.

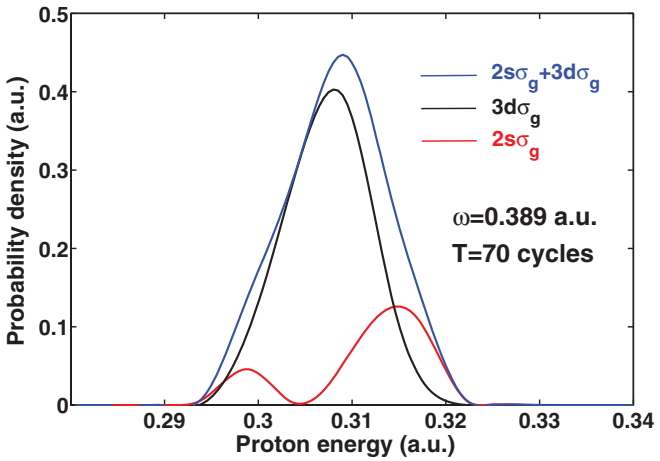

FIG. 8. (Color online) KER of the protons in the dissociative channels $2s\sigma_g$ (red curve), $3d\sigma_g$ (black curve), and the sum of both contributions (blue curve), obtained from the dissociation of the stationary state (vibrational ground state) $1s\sigma_g(v=0)$ in H_2^+. The results are obtained with a 27-fs laser pulse of central frequency $\omega = 0.389$ a.u. and peak intensity $I = 10^{12}$ W/cm^2.

mentioned above, which results from the oscillation of the vibrational Franck-Condon wave packet on the $1s\sigma_g$ potential curve, is now the dominant one. Moreover, the KER spectrum in the $2p\sigma_u$ exhibits a similar interference pattern confirming the predominance of this second mechanism.

Figure 8 depicts the KER of the protons after the two-photon dissociation of the vibrational ground state ($v = 0$) in H_2^+. Again, a clear interference pattern is exhibited in the $2s\sigma_g$ channel. The modulation is a manifestation of an interference effect similar to the one sketched in Fig. 2, but

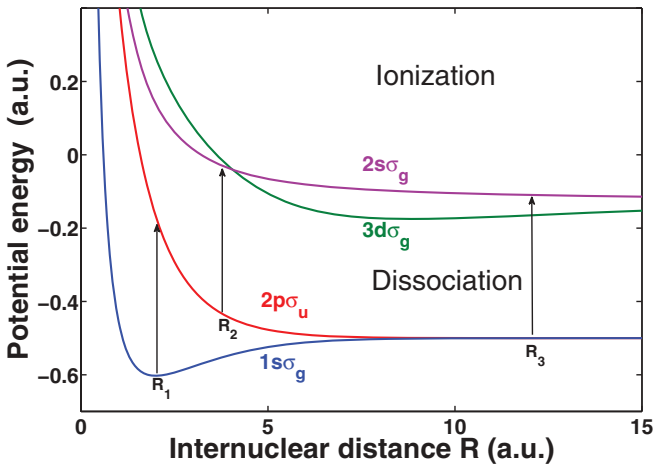

FIG. 9. (Color online) Sketch of a vibrational wave-packet interference process in the $2s\sigma_g$ dissociation channel of H_2^+. A wave packet is created at time $t = 0$ on the $2p\sigma_u$ electronic potential curve by absorption of one photon. Then, as this wave packet moves outwards, to larger values of R, two new wave packets are created on the $2s\sigma_g$ as the result of two subsequent one-photon transitions at $R_2 \sim 3.2$ a.u. and $R_3 \sim 12.8$ a.u. It is the interference between these two wave packets that gives rise to the oscillatory pattern in the kinetic energy distribution of the nuclei shown in Fig. 8.

there is an important difference. In the present context, a wave packet is first launched on the $2p\sigma_u$ potential curve by the absorption of one photon. Then, as this wave packet moves outwards to larger values of R, two new wave packets are created on the $2s\sigma_g$ electronic potential curve in two subsequent one-photon (resonant) transitions, occurring at $R \sim 3.2$ a.u. and $R \sim 12.8$ a.u., respectively (see Fig. 9). It is the interference between these two wave packets that gives rise to the oscillatory pattern in the kinetic energy distribution of the nuclei. Finally we note in Fig. 8 that the contribution of the $3d\sigma_g$ dissociative channel strongly dominates the contribution of the $2s\sigma_g$ channel, therefore the total KER does not show the double peak structure.

IV. CONCLUSION

In this contribution, we study the interaction of a single femtosecond pulse with H_2^+ initially in a superposition of vibrational states resulting from a vertical (Franck-Condon) transition from the H_2 ground state. The objective is twofold: to validate our spectral approach based on Sturmian functions and to analyze the effect of nuclear interferences on the population of the dissociative channels $2s\sigma_g$ and $3d\sigma_g$ in the two-photon dissociation of the molecule. In our spectral approach, we use the prolate spheroidal coordinate system to describe the electronic wave functions in a basis of Laguerre and Legendre functions. We treat the vibrational motion by using a basis of Sturmian functions. Kinetic energy release spectra are calculated and compared with the results obtained with another spectral method based on B splines. Both methods give results that are in very good agreement. We confirm that the vibrational wave packet produced in the $3d\sigma_g$ dissociative channel by a two-photon resonant transition from the $1s\sigma_g$ interferes with the wave packet produced in the $3d\sigma_g$ channel by two resonant one-photon transitions via the $2p\sigma_u$ channel. This interference leads to a double peak structure in the KER spectrum of the protons. On the other hand, various indications suggest that the similar structure observed in the KER spectrum of the protons in the $2s\sigma_g$ channel results from other mechanisms. For photon energies ranging from 0.32 to 0.38 a.u., the oscillations of the initial vibrational wave packet in the $1s\sigma_g$ channel lead to the sequential creation of two wave packets in the $2s\sigma_g$ channels that will eventually interfere. At $\omega = 0.389$ a.u. we have identified a third mechanism leading to interferences; it involves one-photon resonances between the $2p\sigma_u$ and $2s\sigma_g$ potential curves at two different internuclear distances. Finally, we also show that, in the case of a photon energy of 0.32 a.u. and pulse duration of 18 fs, the double peak structure subsists in the KER spectrum of the protons when the contributions from the $2s\sigma_g$ and $3d\sigma_g$ dissociative channels are added together. This is indeed very interesting from the experimental point of view since it is extremely difficult to separate both contributions.

ACKNOWLEDGMENTS

V.M.N gratefully acknowledges the CUD (Commission Universitaire pour le développement de la Communauté Française de Belgique) for financial support through the

MA-1245 PIC (Projet inter-Universitaire Ciblé). He is also indebted to the COST Action CM0702, "Chemistry with ultrashort pulses and free-electron lasers: looking for control strategies through 'exact' computations" for financing two short term scientific missions at the "Centre des Lasers Intenses et Applications," Université Bordeaux 1. M.F. acknowledges support from the Bergen Research Foundation (Norway). The authors thank the Université catholique de Louvain for providing them with access to the supercomputer of the CISM (Calcul Intensif et Stockage de Masse) which is supported by the FNRS (Fonds National de la Recherche Scientifique) through the FRFC (Fonds de la recherche fondamentale collective) Project No 2.4556.99, "Simulations Numériques et traitement des données."

[1] Y. Nabekawa, H. Hasegawa, E. J. Takahashi, and K. Midorikawa, Phys. Rev. Lett. **94**, 043001 (2005).
[2] N. Miyamoto, M. Kamei, D. Yoshitomi, T. Kanai, T. Sekikawa, T. Nakajima, and S. Watanabe, Phys. Rev. Lett. **93**, 083903 (2004).
[3] K. Hoshina *et al*., J. Phys. B **39**, 813 (2006).
[4] R. Nepstad, T. Birkeland, and M. Førre, Phys. Rev. A **81**, 063402 (2010).
[5] A. D. Bandrauk, *Molecules in Strong Fields* (Dekker, New York, 1993).
[6] J. H. Posthumus, Rep. Prog. Phys. **67**, 623 (2004).
[7] Y. Furukawa, Y. Nabekawa, T. Okino, S. Saugout, K. Yamanouchi, and K. Midorikawa, Phys. Rev. A **82**, 013421 (2010).
[8] A. Palacios, S. Barmaki, H. Bachau, and F. Martín, Phys. Rev. A **71**, 063405 (2005).
[9] A. Palacios, H. Bachau, and F. Martín, Phys. Rev. Lett. **96**, 143001 (2006).
[10] M. Førre, S. Barmaki, and H. Bachau, Phys. Rev. Lett. **102**, 123001 (2009).
[11] B. Abeln, J. V. Hernández, F. Anis, and B. D. Esry, J. Phys. B **43**, 155005 (2010).
[12] Hai-Xiang He, Rui-Feng Lu, Pei-Yu Zhang, Ke-Li Han, and Guo-Zhong He, J. Phys. B **45**, 085103 (2012).
[13] G. L. Kamta and A. D. Bandrauk, Phys. Rev. A **71**, 053407 (2005).
[14] S. Barmaki, H. Bachau, and M. Ghalim, Phys. Rev. A **69**, 043403 (2004).
[15] A. Palacios, H. Bachau, and F. Martín, J. Phys. B **38**, L99 (2005).
[16] H. Bachau, E. Cormier, P. Decleva, J. E. Hansen, and F. Martín, Rep. Prog. Phys. **64**, 1815 (2001).
[17] E. Foumouo, G. L. Kamta, G. Edah, and B. Piraux, Phys. Rev. A **74**, 063409 (2006).
[18] J. Eiglsperger, B. Piraux, and J. Madroñero, Phys. Rev. A **80**, 022511 (2009).
[19] J. Eiglsperger, B. Piraux, and J. Madroñero, Phys. Rev. A **81**, 042527 (2010).
[20] J. Eiglsperger, B. Piraux, and J. Madroñero, Phys. Rev. A **81**, 042528 (2010).
[21] S. Barmaki and H. Bachau, J. Phys. B **40**, 463 (2007).